A combination of sugar esters and chitosan to promote *in vivo* wound care

Mattia Tiboni[1#], Enas Elmowafy[2#], Marwa O. El-Derany[3], Serena Benedetti[1], Raffaella Campana[1], Michele Verboni[1], Lucia Potenza[1], Francesco Palma[1], Barbara Citterio[1], Maurizio Sisti[1], Andrea Duranti[1], Simone Lucarini[1], Mahmoud E. Soliman[2,4]*, and Luca Casettari[1]*

[1]*Department of Biomolecular Sciences, University of Urbino Carlo Bo, Piazza del Rinascimento, 6, 61029 Urbino (PU), Italy.*
[2]*Department of Pharmaceutics and Industrial Pharmacy, Faculty of Pharmacy, Ain Shams University, Monazzamet Elwehda Elafrikeya Street, Abbaseyya, Cairo, Egypt, 11566*
[3]*Department of Biochemistry, Faculty of Pharmacy, Ain Shams University, Monazzamet Elwehda Elafrikeya Street, Abbaseyya, Cairo, Egypt, 11566*
[4]*Egypt-Japan University of Science and Technology (EJUST), New Borg El Arab, Alexandria, Egypt, 21934*

*Correspondence: luca.casettari@uniurb.it;. Tel. (Italy): +390722303332

ABSTRACT

In recent years, researchers are exploring innovative green materials fabricated from renewable natural substances to meet formulation needs. Among them, biopolymers like chitosans and biosurfactants such as sugar fatty acid esters are of potential interest due to their biocompatibility, biodegradability, functionality, and cost-effectiveness. Both classes of biocompounds posses the ability to be efficiently employed in wound dressing to help physiological wound healing, which is a bioprocess involving uncontrolled oxidative damage and inflammation, with an associated high risk of infection.

In this work, we synthesized two different sugar esters (*i.e.*, lactose linoleate and lactose linolenate) that, in combination with chitosan and sucrose laurate, were evaluated *in vitro* for their cytocompatibility, anti-inflammatory, antioxidant, and antibacterial activities and *in vivo* as wound care agents. Emphasis on Wnt/β-catenin associated machineries was also set. The newly designed lactose esters, sucrose ester, and chitosan possessed sole biological attributes, entailing considerable belending for convenient formulation of wound care products. In particular, the mixture composed of sucrose laurate (200 μM), lactose linoleate (100 μM), and chitosan (1%) assured its superiority in terms of efficient wound healing prospects *in vivo* together with the restoring of the Wnt/β-catenin signaling pathway, compared with the marketed wound healing product (Healosol®), and single components as well. This innovative combination of biomaterials applied as wound dressing could effectively break new ground in skin wound care.

Keywords:
Antimicrobial; Antioxidant; Anti-inflammatory; Wound dressing; Wnt/β-catenin signaling

1. INTRODUCTION

In recent years, the research of new materials is evolving to different technologies for the introduction and approval of fit-for-purpose ones that can fulfill the unique requirements of novel pharmaceutical and biomedical platforms in use and under development (Guth et al., 2013). From an environmental impact perspective, formulation scientists have strived to explore customized biomaterials, fabricated from renewable natural substances (Lukic et al., 2016; Manzoor et al., 2020).

In this scenario, the development and characterization of new biosurfactants are becoming increasingly appealing. Sugar fatty acid esters are one such class of commodities with striking performance that are securing a considerable share in various industrial segments (Neta et al., 2015; Pérez et al., 2017). The preponderance of these compounds over their chemical counterparts has been evidenced concerning biodegradability, biocompatibility, quality, functionality, and cost-effectiveness (Lucarini et al., 2016; Lukic et al., 2016). Various fatty acid and saccharide moieties were conjugated to form sugar derivatives with high product output and diversity (Neta et al., 2015; Zheng et al., 2015). Their surface activity and emulsifying adequacy have been well-related to the sugar core and esterified fatty acid types, the number of fatty acids, and esterification degree (Gumel et al., 2011; Neta et al., 2012; Teng et al., 2020; Wagh et al., 2012).

It is well posited that these non-ionic surfactants have best exemplified solubilizing agents, permeation enhancers (PEs), stabilizing agents for biologics, as well as integral parts of various delivery platforms (Elmowafy et al., 2020; Kale and Akamanchi, 2016; Klang et al., 2013; Lucarini et al., 2018; McCartney et al., 2021; Schiefelbein et al., 2010; Szuts et al., 2011). In the aspect of biological relevance, sugar esters have been utilized as competent therapeutic entities with biocidal potentiality against pathogens including bacteria, fungi, and viruses (Matin et al., 2020; Zhang et al., 2015; Zhao et al., 2015). Besides, some sugar derivatives have been recognized for their anti-tumor and anti-inflammatory activities (Ferrer et al., 2005; Guan et al., 2019; Marathe et al., 2020). However, the examination of their linked toxicity, at cellular and tissue levels, and cogent *in vivo* studies are still limited and need to be put forward.

Wound healing is a complicated well-tuned bioprocess that involves sequential interlinked hemostasis, inflammation, re-epithelialization, and tissue maturation, critically influencing both patients and healthcare providence (Aldalaen et al., 2020; Tiboni et al., 2021). Excessive and uncontrolled oxidative damage and the subsequent pathological out-of-control inflammation are the underlying causes accountable for postponed and uncoordinated wound healing (Sanchez et al., 2018). Functionalized wound dressings, therefore, should entail adjustable features to actively participate in structural and functional skin reconstruction. Among these, wound dressings based on

chitosan have been extensively utilized featuring biodegradability, long-term stability, and beneficial multimodal activities for wound management (*i.e.*, hemostatic, anti-inflammatory, antimicrobial, antioxidant, and skin regeneration) (Feng et al., 2021; Khan and Mujahid, 2019; Matica et al., 2019; Mohan et al., 2020; Saberian et al., 2021). In clinical translation scope, chitosan-based wound sprays, gels, patches, bandages, and fibres are introduced on the market as safe and easily applied biopolymer wound dressings (Matica et al., 2019).

In principle, it has been plausible to hypothesize that these biomaterials could break new ground in skin wound care. Accordingly, sugar esters based on lactose with two fatty acids [*i.e.*, linoleic and linolenic acids, namely lactose linoleate (C18:2ω) and lactose linolenate (C18:3ω), respectively] were synthesized, and their aptness for mitigating skin lesions and infections was elucidated. Further, their potential was compared and associated with the commercially available sucrose laurate (C12), and with chitosan. To evaluate the potential impact of the present study in a therapeutic application, we explored *in vitro* antioxidant, anti-inflammatory, and antimicrobial properties followed by an *in vivo* wounding model study. Dermal matrices with binary and triple combinations of these sugar esters and chitosan have been designed and probed as well. Healosol®, a marketed spray product containing phenytoin, was used for comparative purposes. In fact, when topically applied, phenytoin was well-reported to promote wound healing via prompting fibroblast proliferation and collagen deposition and possessing antibacterial efficacy (Anstead et al., 1996; Shaw et al., 2007).

In support of our hypothesis, the underlying mechanistic impact of the utilized biomaterials on wound healing was assessed *via* profiling the expression of the genes of Wnt/β-catenin signaling pathway using reverse transcription-quantitative real-time polymerase chain reaction (RT-qPCR). Supporting evidences have confirmed the vital role played by the Wnt/β-catenin signaling pathway in wound healing at the molecular level (Amini-Nik et al., 2014; Yang et al., 2017; Zhang et al., 2018). Indeed, canonical Wnt signaling via β-catenin and its target c-myc are critically involved in cell migration, invasion, proliferation, and inflammatory events during the wound healing process (Lamouille et al., 2014). Interestingly, recent reports showed that natural compounds including chitosan might modulate Wnt/β-catenin signaling in various diseases (Hu et al., 2018; Sferrazza et al., 2020). To the best of the authors' knowledge, no data on the functional contributes of these innovative wound healing frontiers are available. Additionally, the effect of sugar esters and chitosan on the stringent control of the molecular expressions of key factors in Wnt/β-catenin signaling that affects wound healing is far from clear.

2. MATERIALS AND METHODS

2.1 Materials

Chitosan chloride (Chitoceuticals® Chitosan HCl code 54040) was purchased from Heppe Medical Chitosan GmbH (Halle, Germany), linolenic and linoleic acids from Fluorochem (Hadfield, UK), triethylamine (Et3N) anhydrous from TCI (Zwijndrecht, Belgium), lactose monohydrate and 4-(dimethylamino)pyridine (DMAP) from Carlo Erba (Milan, Italy). Sucrose monolaurate, *p*-toluenesulfonic acid, 2,2-dimethoxypropane, 1-(3-dimethylaminopropyl)-3-ethylcarbodiimide hydrochloride (EDCI·HCl), tetrafluoroboric acid diethyl ether complex ($HBF_4 \cdot Et_2O$), carbonyl cyanide 4-(trifluoromethoxy) phenylhydrazone (FCCP), and all organic solvents used were purchased from Sigma-Aldrich (Milan, Italy). Healosol® spray (phenytoin) was obtained from the Egyptian company for advanced pharmaceuticals (Egypt). Prior to use dichloromethane (CH_2Cl_2) was dried with molecular sieves with an effective pore diameter of 4 Å. The structure of compounds was unambiguously assessed by MS, ^{1}H NMR, and ^{13}C NMR. ESI-MS spectra were recorded with a Waters Micromass ZQ spectrometer in a negative or positive mode using nebulizing nitrogen gas at 400 L/min and a temperature of 250 °C, cone flow 40 mL/min, capillary 3.5 kV, and cone voltage 60 V; only molecular ions $[M-H]^-$, $[M+NH_4]^+$ or $[M+Na]^+$ are given. ^{1}H NMR and ^{13}C NMR spectra were recorded on a Bruker AC 400 or 101, respectively, spectrometer and analyzed using the TopSpin 1.3 software package. Chemical shifts were measured by using the central peak of the solvent. Column chromatography purifications were performed under "flash" conditions using Merck 230–400 mesh silica gel. TLC was carried out on Merck silica gel 60 F254 plates, which were visualized by exposure to ultraviolet light and to an aqueous solution of ceric ammonium molybdate.

2.2 Methods

2.2.1 Synthesis of lactose-based surfactants

2.2.1.1 General procedure for the synthesis of lactose tetra acetate monoesters 6′-*O*-octadec-9*Z*-12*Z*- dienoyl- and 6′-*O*-octadec-9*Z*-12*Z*-15*Z*-trienoyl-4-*O*-(3′,4′-*O*-isopropylidene-β-D-galactopyranosyl)-2,3:5,6-di-*O*-isopropylidene-1,1-di-*O*-methyl-D-glucopyranose (**3a,b** – Scheme 1).

DMAP (0.048 g, 0.4 mmol) and linoleic acid (**1a**) or linolenic acid (**1b**) (2 mmol) were added to a solution of 4-*O*-(3′,4′-*O*-isopropylidene-β-D-galactopyranosyl)-2,3:5,6-di-*O*-isopropylidene-1,1-di-*O*-methyl-D-glucopyranose (lactose tetra acetate, LTA) (**2**) (1.22 g, 2.4 mmol) in dry CH_2Cl_2 (20.0 mL) at room temperature under N_2 atmosphere. The mixture was cooled at 0 °C and added of Et_3N (2.4 mmol, 0.334 mL) and EDCI·HCl (0.460 g, 2.4 mmol), then stirred at 0 °C for 10 minutes and at

room temperature for 3 days, diluted with CH_2Cl_2, and washed with saturated aqueous NH_4Cl and $NaHCO_3$ solutions. The organic phase was dried on Na_2SO_4, filtered, and concentrated. Purification of the residue by column chromatography (cyclohexane/EtOAc 7:3) gave **3a,b** as a pale yellow oil.

2.2.1.2 General procedure for the synthesis of lactose fatty acid monoesters 6′-*O*-octadec-9*Z*-12*Z*-dienoyl- and 6′-*O*-octadec-9*Z*-12*Z*-15*Z*-trienoyl-4-*O*-(β-D-galactopyranosyl)-D-glucopyranose (**4a,b**).

Compounds **3a** or **3b** (0.38 mmol) were dissolved in H_2O (0.030 mL) and CH_3CN (3 mL), $HBF_4{\cdot}Et_2O$ (0.006 mL) was added and the mixture was stirred at 0 °C for 5 h. The white solid precipitated was filtered, washed with CH_3CN and dried. Trituration with petroleum ether gave **4a,b** as white solids.

Yields, ESI-MS, and NMR characterizations are reported in the supplementary material.

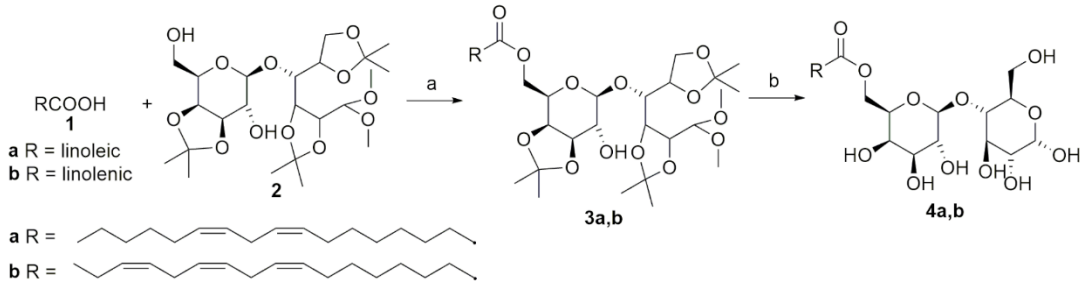

Scheme 1. Reagents and conditions: (a) EDCI·HCl, DMAP, dry TEA, dry CH_2Cl_2, 0 °C 10' then r.t. 72 h; (b) $HBF_4{\cdot}Et_2O$, H_2O, CH_3CN, 0 °C, 5 h.

2.2.2 Cell culture

HaCaT (immortalized human keratinocytes) and RAW 264.7 (murine macrophages) cell lines were used to investigate the biological properties of chitosan and sugar-based esters. Cells were grown in Dulbecco's modified eagle's medium (DMEM) medium supplemented with 10% fetal bovine serum, 1% L-glutamine, and 1% penicillin/streptomycin 100 U/mL, and maintained in a CO_2 incubator at 37 °C and 5% CO_2. Cell culture reagents were from Sigma-Aldrich (Milan, Italy).

2.2.3 Cell viability assays

HaCaT cell viability after chitosan and sugar-based ester administration was analyzed by water-soluble tetrazolium (WST)-8 and sulphorodamine B (SRB) assays, which evaluate cell metabolic activity and cell protein content, respectively. Briefly, cells ($5x10^3$/well) were seeded in 96-well plates and treated for 2 h with chitosan (0.01-1%) or sugar-based esters (6.25-200 μM). Test compounds were then removed and fresh medium added. After 24 h of incubation, WST-8 (Sigma-

Aldrich, Milan, Italy) was added to each well, and cells were further incubated at 37 °C up to 4 h (Catalani et al., 2017b). Color development was monitored at 450 nm in a multiwell plate reader (BioRad Laboratories, Hercules, USA). In the same 96-well plate, the SRB test was then performed, as previously published (Farabegoli et al., 2017). Briefly, cell culture medium was removed, cells fixed with 50% trichloroacetic acid for 1 h at 4 °C, rinsed with water, and incubated for 30 min with 0.4% SRB solution (Sigma-Aldrich, Milan, Italy). After rinsing with 1% acetic acid and solubilizing in 10 mM Tris for 10 min, absorbance was measured at 570 nm in a microplate reader (BioRad Laboratories, Hercules, USA). Data were expressed as cell growth (%) versus non-treated cells (controls).

2.2.4 Nitric oxide detection

The anti-inflammatory properties of chitosan and sugar-based esters were evaluated in RAW 264.7 cells stimulated by lipopolysaccharide (LPS, Sigma-Aldrich, Milan, Italy). Briefly, cells ($3x10^4$/well) were seeded in 96-well plates and treated for 2 h with chitosan (0.01-0.5%) or sugar-based esters (25-50 μM). Test compounds were then removed and cells stimulated with 1 μg/mL LPS for 24 h. After incubation, nitric oxide (NO) levels were determined in the medium by mixing equal volumes of supernatant and Griess reagent (Sigma-Aldrich, Milan, Italy) (Bryan and Grisham, 2007). Absorbance was measured at 570 nm using a plate reader (BioRad Laboratories, Hercules, USA). In the same 96-well plate, an SRB test was also performed as described above, to evaluate RAW 264.7 cell viability after LPS treatment.

2.2.5 Evaluation of antioxidant properties (DPPH and DCFH-DA assays)

The ability of chitosan and sugar-based esters to act as antioxidants was evaluated by the 2,2-diphenyl-1-picryl-hydrazyl-hydrate (DPPH) radical scavenging assay, as previously described (Saltarelli et al., 2019). Chitosan was solubilized and diluted in water (tested concentrations 0.01-1%), while sugar-based esters were first dissolved in dimethyl sulfoxide (DMSO) and then diluted in ethanol (EtOH) (tested concentrations 6.25-200 μM). DPPH (100 μM, Sigma-Aldrich, Milan, Italy) was prepared in EtOH. The scavenger effect was expressed as % = [(OD 517 nm control - OD 517 nm sample /OD 517 nm control] x 100. EC_{50} values (*i.e.*, the concentration required to obtain a 50% antioxidant effect) werethen calculated.

Moreover, the antioxidant properties of chitosan and sugar-based ester were analyzed in HaCaT cells by 2',7'-dichlorofluorescin diacetate (DCFH-DA, Sigma-Aldrich, Milan, Italy), which turns to highly fluorescent 2',7'-dichlorofluorescein (DCF) upon oxidation (Catalani et al., 2017a). Briefly, cells ($1x10^4$/well) were seeded in black 96-well plates and incubated for 2 h with chitosan (0.01-

1%) or sugar-based esters (100 μM). Test compounds were then removed and DCFH-DA (5 μM) added to each well for 30 min at 37 °C. After excess probe removal, cells were treated with hydrogen peroxide (H_2O_2, 100 μM) for 30 min and DCF fluorescence emission measured at ex/em 485/520 nm in the multiwell plate reader FluoStar Optima (BMG Labtech, Germany). Data were expressed as relative oxidation versus non-oxidized cells.

2.2.6 DNA nicking assay

The protective effect of chitosan and sugar-based esters against DNA oxidative damage was evaluated by the DNA nicking assay, which employs ferrous ions and dioxygen (Fe^{2+} + O_2) to generate free radical-induced DNA strand breaks. A cell-free system composed of supercoiled pEMBL8 plasmid DNA, which resembles the structure of mtDNA, was used(Mari et al., 2018). Briefly, plasmid DNA (5.8 μg/mL) was incubated in PBS in the presence of different amounts of sugar-based surfactants (from 1.2 mM to 40 μM) or chitosan (from 0.5% to 0.02% w/v) in a volume of 72 μL. DNA damage was generated by adding 8 μl of freshly made 3 mM ferrous sulphate (final Fe^{2+} = 300 μM), and after 10 minutes, the reaction was stopped by adding 40 μL of Orange G loading buffer. The disappearance of the supercoiled form of the plasmid was assessed on an ethidium bromide-stained agarose gel electrophoresis followed by the quantitation by Gel Doc 2000 and Quantity One software (Bio-Rad). The EC_{50} values were calculated determining the concentration of the compound that protects half of the supercoiled plasmid.

2.2.7 Microorganisms culture conditions

In this study, several strains of human clinical isolates of *Staphylococcus aureus* [*S. aureus* HCS026, *S. aureus* 2/5, *S. aureus* 28/10, *S. aureus* 18/9, *S. aureus* HCS002 methicillin-resistant (MRSA)], as well as the clinical isolate *Pseudomonas aeruginosa* C86, belonging to the strain collection of Pharmacology and Hygiene Division (Department of Biomolecular Sciences, University of Urbino), were used. The reference strains, *S. aureus* ATCC 43387, *S. aureus* ATCC 43300 and *P. aeruginosa* ATCC 27583 were also included. All the *S. aureus* strains were cultured in Tryptone soy agar (TSA) (VWR, Milan, Italy) and subcultured in Mannitol Salt Agar (MSA) (VWR) at 37°C for 24 h, while *Pseudomonas* strains were grown in Cetrimide agar (VWR) at the same culture conditions; all the strains were stored at -80 °C in Nutrient broth (VWR) supplemented with 20% glycerol.

Pathogenic filamentous dermatophytes belonging to the strain collection of Pharmacology and Hygiene Division (Department of Biomolecular Sciences, University of Urbino) (*Trichophyton mentagrophytes* F6, *Trichophyton rubrum* F2, *Trichophyton violaceum* F11, *Epidermophyton*

floccosum F12) and the reference strain *Candida albicans* ATCC 10231 were also included. The dermatophytes were maintained on Potato Dextrose Agar (PDA) (VWR) at 35°C for 7 days, while *C. albicans* at 37 °C for 24 h.

2.2.8 Minimum inhibitory concentration and checkboard

For each molecule, the minimum inhibitory concentration (MIC) was determined following the standard microdilution method (Clinical and Laboratory Standards Institute CLSI, 2017). For filamentous fungi and mycete the conidial suspensions were prepared according to the CLSI M38-A and CLSI M27-A protocol respectively.

At first, each compound was dissolved (5 mg/mL) in DMSO of biological grade (Sigma, Milan, Italy) to obtain concentrated stock solutions. In the case of sucrose laurate, the stock solution was prepared in distilled water and then 0.22 µm filtered. Preliminary assays were performed to exclude the possible bacteriostatic and/or bactericidal activity of the solvent; in any case, the volume of DMSO never exceeded 5% (v/v) of the final total volume. Chitosan was dissolved in water with 1% acetic acid to a final concentration of 4% (w/v) and left overnight at 70 °C with gentle stirring. Afterward, the solution was autoclaved at 121 °C for 15 min and then maintained at room temperature until use.

One colony of each bacterial strain was inoculated in 10 mL of Tryptone Soy Broth (TSB) (VWR) and incubated at 37 °C for 18 h. The bacterial suspensions were adjusted to about 10^6 CFU/mL (OD $_{610nm}$ 0.13-0.15) in Mueller Hinton Broth II (MHB II) (VWR) and 100 µL was added to wells of the 96-well plate together with the appropriate volumes of each sugar-based monoester solution (from 2048 to 16 µg/mL). In the case of chitosan, the used concentrations ranged from 2% to 0.25%. Two rows were used as positive and negative controls inoculating bacteria alone and MHB II alone respectively. MIC was defined as the lowest concentration of compound able to inhibit bacterial growth after 24 h of incubation at 37 °C. All data were expressed as the mean of three independent experiments performed in duplicate.

As regards the filamentous fungi, spores were harvested from PDA plate by adding 2 mL of sterile 0.85% saline solution supplemented with 0.05% Tween 80; the surface was scraped with a sterile cotton swab, and the suspension was transferred in a sterile tube and left at room temperature for 5 min to allow the sedimentation of hyphal fragments. Afterward, the homogeneous upper suspension was vortexed for 15 s and adjusted to an optical density (OD 530 nm) between 0.09 and 0.4 corresponding to about 10^6 spores/mL. For *C. albicans* the mixture suspension was adjusted with a spectrophotometer to a turbidity of 0.12 (about 10^7 cfu/mL). Successively, 100 µL of each fungal suspension was diluted 1:50 in standard RPMI 1640 medium (Sigma) and inoculated into 96-well

plates together with the appropriate volumes of each test solution as described above. Two rows were left for positive control growth and negative controls (medium only), respectively. Undecylenic acid was used as internal control molecule. Plates were incubated at 35 °C for dermatophytes and 37 °C for 48 h for *C. albicans* and examined after 48 h of incubation. MIC is defined as the lowest drug concentration that inhibits visible growth in comparison with the control (untreated sample). In addition, the turbidity of the 96-wells plate was assessed by spectrophotometer (530 nm) (Multiskan EX, Thermo Scientific, Italy).

The synergy of the most active sugar-based monoester (sucrose laurate) and chitosan against representative bacterial strains chosen based on their MIC values (*S. aureus* 2/5, *S. aureus* 18/19 and *P. aeruginosa* C86) was evaluated by the checkerboard method. The interactions between the combinations of sucrose laurate and chitosan were indicated by the fractional inhibitory concentration (FIC) index for each compound. The former was performed using 2-fold increasing concentrations of each compound (from the related MIC values up to 8 µg/mL) and chitosan (from 1% to 0.25% v/v). In the case of the compounds dissolved in DMSO, the upper limit of the concentrations range tested was determined considering a final concentration of 1% DMSO. The value of FIC index was interpreted as follows: ≤ 0.5, synergy; > 0.5 and ≤ 1.0, additive; > 1.0 and < 4, indifferent; ≥ 4, antagonistic.

2.2.9 Haemolysis Assays

The haemolysis of compounds was evaluated as described by Chongsiriwatana et al. (Chongsiriwatana et al., 2008). Briefly, 4 mL of freshly drawn, heparinized human blood was diluted with 25 mL of phosphate buffered saline (PBS), pH 7.4. After washing three times in 25 mL of PBS, the pellet was resuspended in PBS to ~20 vol %. A 100 µL amount of erythrocyte suspension was added to 100 µL of different concentrations of the most active sugar-based monoesters and chitosan respectively (starting from the related MIC values). PBS and 0.2 % Triton X-100 were used as negative and positive control, respectively. Each condition was tested in triplicate. After 1 h of incubation at 37 °C each well was centrifuged at 1200 G for 15 min, the supernatant was diluted 1:3 in PBS and transferred to a new plate. The OD_{350} was determined using the Synergy HT microplate reader spectrophotometer (BioTek, Winooski, VT, USA).

The haemolysis (%) was determined as reported in Eq. 1:

$$[(A - A_0)/(A_{total} - A_0)] \times 100 \quad (1)$$

where A is the absorbance of the test well, A_0 the absorbance of the negative control, and A_{total} the absorbance of the positive control; the mean value of three replicates was recorded.

2.2.10 Stability to serum protease

The sugar-based monoesters and the chitosan were pre-incubated in fresh 50% blood plasma solution for 0, 3, and 6 hours at 37 °C (Chongsiriwatana et al., 2008). Briefly, a representative bacterial strain (*i.e.*, *S. aureus* ATCC 43300) was grown for 6 h in BH broth and diluted in Mueller Hinton II (Oxoid, Milano, Italy) to give a final concentration of $1.5x10^6$ CFU/mL. Fresh human blood cells were centrifuged at 3000 rpm for 5' to separate the plasma from the red blood cells. For the selected sugar-based monoesters three aliquots were dissolved in DMSO at a concentration of 2048 μg/mL and diluted 2-fold in the plasma to reach the final concentration of 1024 μg/mL. In the case of chitosan, it was 2-fold diluted in the plasma to reach the final concentration of 1%. The samples were incubated at 37 °C for 0, 3, and 6 h and then used to perform MIC assays according to the broth microdilution method in 96-well microtiter plates, as mentioned above. No difference of MIC values among the trials performed in different plasma-preincubation times attests the plasma stability.

2.2.11 *In vivo* wound healing model

2.2.11.1 Animals used

Seventy-two male Wistar albino rats weighing 150-180 g were used for *in vivo* study. The rats were provided with a standard normal diet and drinking water during the experiment. Rats were caged in open cages at 25 °C with 12 h light and dark cycles at the animal facility of the Faculty of Pharmacy (Ain Shams University, Egypt) and were left for one week for acclimatization before starting the experiment. All animal experimental work was approved by the Ethics Committee at the Faculty of Pharmacy, Ain shams university, Egypt, and conducted according tothe U.K. Animals (Scientific Procedures) Act, 1986 and the EU Directive 2010/63/EU guidelines for animal studies.

2.2.11.2 Wound excision model

Wounds were induced on the sterilized shaved dorsal skin of rats after being anesthetized using intraperitoneal (IP) ketamine (50 mg/kg). One circular excision wound was induced with blunt dissection (20 mm in diameter) and the wound was left exposed.

2.2.11.3 Experimental design

The experimental model duration was fifteen days. The study included twelve equal groups of rats, each group consisting of six rats. The appraisal of delivery potential of chitosan, sucrose laurate, lactose linoleate, and lactose linolenate, either alone or their dual and triple combinations was explored on wound healing. The therapeutic effect of the proposed wound care products was compared with that of the marketed wound healing product (Healosol®). The twelve experimental groups were coded as reported in supplementary material Table 1. The wounds were induced on the upper side of the dorsal skin received the treatment, while the control group was unwounded rats. The formulations under investigation were topically applied on the formed wounds daily for 15 days at the concentrations reported in supplementary material Table 1. For each group, photography of wounds was performed using a digital camera on days 3.5, 7, and 15. The wound condition and percentage of wound healing were recorded via measuring the diameter of the wound in mm.

Two weeks after wound induction, rats were sacrificed by cervical dislocation; skin tissues were excised at the wound areas and washed with ice-cold saline. Afterward, parts of tissues were stored at -80 ˚C until RNA extraction for assessment of gene expression, while the other parts were immediately immersed in appropriate buffer for histological examination and staining.

2.2.12 Histopathological assessment and collagen quantification

Rats were euthanized and the formed granulation tissue was excised leaving a 5 mm margin of normal skin. Skin samples were flushed and fixed in 10% neutral buffered formalin for 72 h. Samples were trimmed and processed in serial grades of ethanol, cleared in xylene, samples were infiltrated and embedded into Paraplast tissue embedding media. 4 µm thick tissue sections were cut by rotatory microtome for demonstration of skin layers in different samples.

Tissue sections were stained by Hematoxylin and Eosin (H&E) as a general morphological examination staining method and examined by using a light microscope (Leica Microsystems GmbH, Wetzlar, Germany) and lesions were recorded. Microscopic examination lesion score system was adopted blind to the treatment conditionsas previously described (Al-Sayed et al., 2020).

Furthermore, tissue sections from all groups were stained by Trichrome stain kit to stain collagenous connective tissue fibers, then examined by using a light microscope (Leica Microsystems GmbH, Wetzlar, Germany). Six non-overlapping fields were randomly selected and scanned from dermal layers of each sample for the determination of area percentage of reactive collagen fibers to Masson’s trichrome stain in six tissue samples. All light microscopic examination

and data were obtained by using the Leica Application module for histological analysis attached to Full HD microscopic imaging system (Leica Microsystems GmbH, Germany).

2.2.13 Reverse transcription-quantitative real-time polymerase chain reaction(RT-qPCR)

Determination of gene expression of Wnt/β-catenin signaling pathway involved in wound healing was done using RT-qPCR. The expression of wingless-type MMTV integration site family1 (Wnt1),Wnt 2, c-myc, and beta-catenin (β-catenin) genes were measured and normalized to β-actin gene asreference gene. Sequences of PCR primer sets used are shown in supplementary material Table 2.

Total RNA was extracted from the wound tissue using Trizol (Thermo Scientific co., USA). Subsequently, RNA was reversely transcribed using a high-capacity cDNA Synthesis Kit (Thermo Scientific co., USA). RT-qPCR was performed using an ABI 7500 RT-PCR System (Applied Biosystems, Foster City, CA, USA). The relative quantification was then calculated by the $2^{-\Delta\Delta Ct}$ method.

2.2.14 Statistical analysis

Comparisons between multiple means were performed via ANOVA followed by post hoc analysis for significance (Tukey test). The level of significance was set at $p < 0.05$. Statistics were performed using GraphPad Prism 6.0 (GraphPad Software, Inc., San Diego, CA, USA).

3. RESULTS AND DISCUSSION

3.1 Lactose esters synthesis and chitosan characterization

The synthesis of lactose linoleate (**4a**) and lactose linolenate (**4b**) was conducted as described in scheme 1. For the coupling reaction of the acids (**1**) with LTA (**2**) (Hough et al., 1979) a modified Steglich esterification (Neises and Steglich, 1978) (EDCI coupling as agent instead of DCC) was found to be the most effective procedure to obtain the products **3a,b** in pure form. In fact, by using the Lypozyme® approach, which requires a high temperature (75 °C) for a relative long time (12 h) (Perinelli et al., 2018) or the activation of the acid as acyl chloride (Campana et al., 2019), which utilizes aggressive thionyl or oxalyl chlorides, several isomerizations of the double bonds in the corresponding linoleate and linolenate esters **3a,b** were observed. Finally, a classical deprotection of LTA-esters **3a,b** was carried out by using catalytic $HBF_4{\cdot}Et_2O$ (McCartney et al., 2021) to obtain the desired free sugar esters **4a,b** in good yield.

Chitosan HCl was characterized using a GPC-SE chromatography reporting a number average (Mn) of 133,285 and a weight average (Mw) of 159,310 with a polydispersity (PDI) of 1.195.

3.2 Chitosan and sugar-based esters showed comparable *in vitro* HaCaT cell compatibility profile

HaCaT cell viability after chitosan and sugar-based ester administration was analyzed both by WST-8 (Figure 1 and supplementary material Table 3) and SRB (Supplementary material Figure 1 and SM Table 4) assays, leading to comparable results. Referring to chitosan, no cytotoxic effects were observed on cell growth with chitosan concentrations between 0.01 and 0.1%. It is worth mentioning that results obtained with higher concentrations; 0.5 and 1% were excluded due to interferences with the assays. As regards sugar-based esters, sucrose laurate promoted significant cell growth at all tested concentrations, while lactose linoleate and lactose linolenate showed suppression of cell viability, reaching < 80% cell viability only at the maximum tested dose (200 μM).

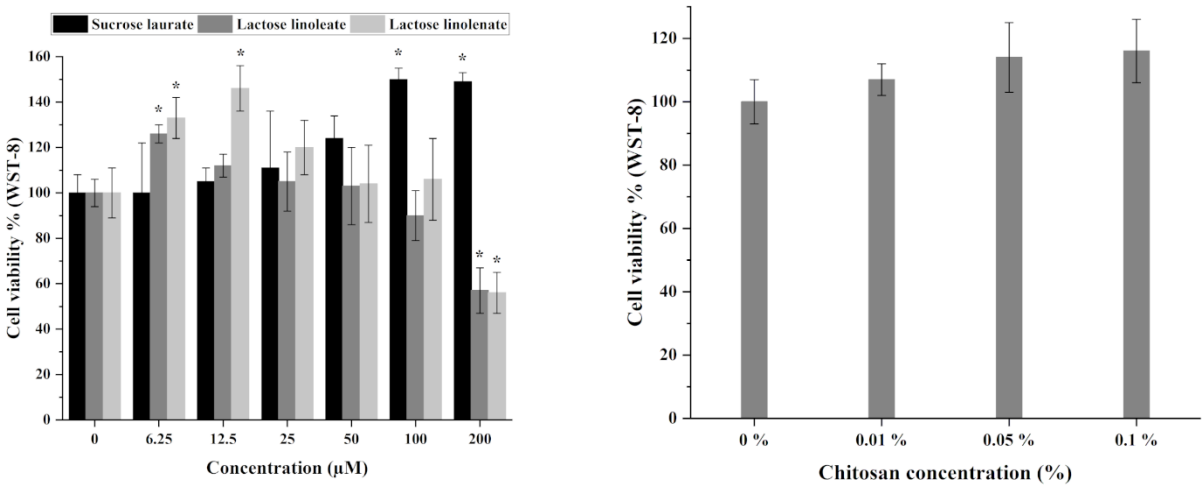

Figure 1. HaCaT cell viability after chitosan and sugar-based ester administration evaluated with WST-8 assay.

3.3 Antioxidant and radical scavenging properties of chitosan and sugar-based esters by DPPH, DCFH-DA, and DNA nicking assays

The radical scavenging ability of chitosan and sugar-based esters evaluated by the DPPH assay is reported in supplementary material Table 5. Chitosan 0.5 and 1% presented a weak but significant scavenger effect against the DPPH radical (EC_{50} equal to 6.93±0.54%). Sucrose laurate did not show appreciable antioxidant properties within the range of concentrations tested. This finding was previously reported, where sucrose laurate was reported to negatively affect the scavenging performance of some natural products (Kim et al., 2009).

On the other side, lactose linoleate and lactose linolenate had EC_{50} values equal to 407±11 µM and 396±8 µM, respectively.

Regarding the DNA nicking assay, the ability of sugar based surfactants and chitosan to protect plasmid DNA was evaluated quantitatively on supercoiled pEMBL8 and expressed as EC_{50}. Sucrose laurate showed no protection (EC_{50} > 3 mM), while lactose linoleate and lactose linolenate moderately protected DNA with EC_{50}values of 0.51±0.08 mM and 0.60±0.07 mM, respectively. At the same time, the presence of chitosan interfered with DNA electrophoresis, thus we were not able to determine its EC_{50} value.

As indicated in Figures 2A, and B, H_2O_2 administration (CTR+) to HaCaT cells led to a significant increment of DCF fluorescence emission as compared to untreated cells (CTR-). When cells were pre-treated for 2 hours with chitosan 0.01-0.1%, a significant reduction of H_2O_2-induced oxidation was observed (Figure 2A, *p <0.05 vs. CTR+). However, results obtained with chitosan 0.5 and 1% were excluded due to interferences with the assay. When cells were pre-treated for 2 hours with

sugar-based esters 100 µM (Figure 2B), no appreciable decrement of H_2O_2-induced oxidation was revealed.

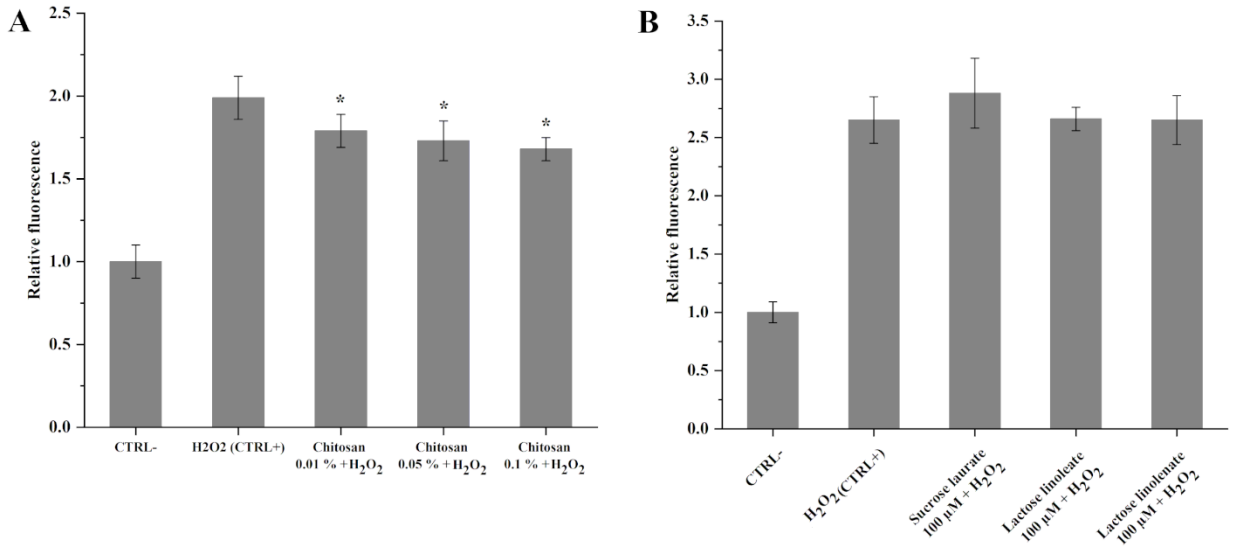

Figure 2. Evaluation of the antioxidant properties of chitosan and sugar-based esters in HaCaT cells

3.4 Chitosan and sugar-based esters manifested anti-inflammatory features in RAW 264.7 cells

As reported in Figure 3, the administration of LPS to RAW 264.7 cells led to NO production and release in the culture medium, while NO could not be quantified in untreated control cells. When cells were pre-treated for 2 hours with chitosan 0.1 and 0.5%, a significant reduction of LPS-induced NO release was observed (Figure 3A). However, the evaluation of cell viability by SRB test revealed that NO reduction was due to a parallel decrement of cell growth (Supplementary material Figure 2A). At non toxic concentrations (0.01 and 0.05%), chitosan did not significantly reduce NO release. In fact, the anti-inflammatory properties of chitosan and NO production is directly related to its molecular weight. Whereas, larger chitosans were found to significantly inhibit the NO production, on the other hand smaller chitosans significantly increase NO production (Chang et al., 2019).

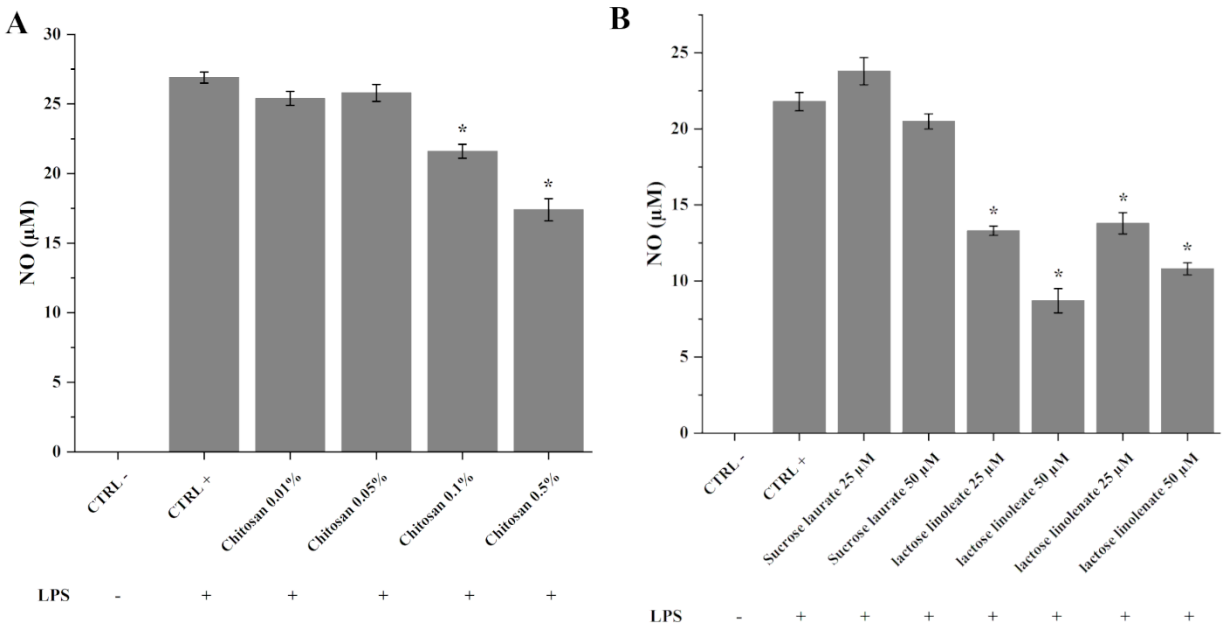

Figure 3. Evaluation of the anti-inflammatory properties of chitosan and sugar-based esters in RAW 264.7 cells. *p <0.05 vs. CTRL +.

Referring to sugar-based esters, a significant reduction of LPS-induced NO release was observed in RAW 264.7 cells pre-treated for 2 hours with lactose linoleate and lactose linolenate (Figure 3B). However, the evaluation of cell viability by SRB test revealed that NO reduction by lactose linoleate was partially due to a concomitant decrement of cell growth (Supplementary material Figure 2B). Sucrose laurate did not affect NO release; therefore, at the concentrations tested, lactose linolenate was the only sugar-based ester revealing anti inflammatory properties without presenting cytotoxic effects.

The incubation of RAW 264.7 cells with chitosan (0.01-0.5%) or sugar-based esters (25-50 µM) alone was not associated with NO release in the extracellular medium (data not shown).

3.5 Evaluation of antimicrobial and antifungal effects of chitosan and sugar-based esters

Data on the antibacterial activity of the examined compounds are summarized in Table 1. As expected, chitosan revealed antimicrobial activity against all the tested microorganisms with MIC values ranging between 1 and 2% (w/v) due to its wide range of antibacterial activities (Abd El-Hack et al., 2020). As regards the sugar-based monoesters, lactose linolenate exhibited MIC values of 1024 µg/mL against notmethicillin-resistant *S. aureus* strains (*S. aureus* HCS026, *S. aureus* 2/5, *S. aureus* 28/10, *S. aureus* 18/9, and *S. aureus* ATCC 43387), resulting in efficacy against the MRSA strains (*S. aureus* HCS002 and *S. aureus* ATCC 43300) and *P. aeruginosa* strains. Sucrose laurate evidenced the greatest antimicrobial activity, reaching the lowest MIC values (256 µg/mL) against *S. aureus* HCS026, *S. aureus* 28/10, *S. aureus* 18/9 and *S. aureus* ATCC 43387. This

finding agreed with recent reports that highlighted a potent antimicrobial activites for sucrose fatty acid estres as sucrose monolaurate due to its physical properties, which effect on the wettability of solids that inturns alteres the adhesion of microorganisms to the surface (Krawczyk, 2018).

The possible synergy between the most active sugar-based monoesters (sucrose laurate) and chitosan was also determined. In most cases, the obtained fractional inhibitory concentration index (FICI) indicate an "indifferent" effect of the molecules between them (FICI = 2), and only in the case of *S. aureus* 28/10 an additive effect has been observed (FICI = 0.75) (data not shown).

Table 1. Antimicrobial activity of chitosan and sugar-based monoesters assessed against *S. aureus* and *P. aeruginosa* strains.

	Chitosan (%)	Sucrose laurate (µg/mL)	Lactose linoleate (µg/mL)	Lactose linolenate (µg/mL)
***S. aureus* HCS026**	2	256	1024	1024
***S. aureus* 2/5**	1	1024	>1024	1024
***S. aureus* 28/10**	1	256	>1024	1024
***S. aureus* 18/9**	1	256	>1024	1024
***S. aureus* MRSA HCS002**	1	1024	>1024	>1024
***S. aureus* ATCC 43300**	1	1024	>1024	>1024
***S. aureus* ATCC 43387**	2	256	1024	1024
***P. aeruginosa* C86**	2	1024	>1024	>1024
***P. aeruginosa* ATCC 27583**	1	1024	>1024	>1024

Data on antifungal activity of the examined compounds are summarized in supplementary material Table 6. Chitosan revealed to be active against all the tested microorganisms with MICs ranging between 1 and 2% (w/v), while sugar-based surfactants (e.g. lactose linolenate and sucrose laurate) showed antifungal activity with MIC between 128 µg/mL and 256 µg/mL in the case of *T. mentagrophytes* F6, *E. floccosum* F12 and *C. albicans*, higher than 521 µg/mL for the other strains. Among the tested molecules, sucrose monolaurate showed the greatest antifungal activity with MICs ranging from 128 µg/mL to 256 µg/mL.

3.6 Evaluation of chitosan and sugar-based esters *in vitro* blood compatibility profile and stability in plasma

The toxicity of these compounds toward mammalian cells was assessed determining their ability to lyse human erythrocytes (Supplementary material Table 7). As shown, chitosan (from 1 to 0.25%) showed very low haemolytic activity with values ranging from 2.97% to 1.53%; similarly, lactose linolenate resulted to be not toxic with haemolytic activity of 5.6% at its MIC value (1024 μg/mL), up to haemolytic activity of 0.73% at lower concentration. On the contrary, sucrose laurate was able to lyse human erythrocytes up to a concentration of 256 μg/mL (haemolytic activity 12.09%), exhibiting low extent of haemolytic activity (1.8%) at lower concentration (128 μg/mL).

As regards the stability to serum proteases (Supplementary material Table 8), the MIC of chitosan, sucrose laurate, and lactose linolenate against *S. aureus* ATCC 43300 in 50% blood plasma, resulted unvaried compared to the initial values, showing no loss of activity in a physiologically relevant time frame of 6 h. In contrast, the MICs values of lactose linoleate were found to be higher (>1024 μg/mL) compared to the initial value (1024 μg/mL), an index of antimicrobial activity reduction.

3.7 *In vivo* studies

3.7.1 Sugar-based esters and their combinations with chitosan decreased the wound area and accelerated wound closure.

The gross appearances of the excision wounds in different groups were visualized at 3, 5, 7, and 15 days after injury (Supplementary material Figure 3). Obviously, on day 15, the untreated skin wound (group II) naturally heal, however, there was still an unclosed wound. The healing process was faster when the tested wound care solutions (*i.e.*, lactose linoleate, lactose linolenate, and chitosan, both in single and mixed forms) were applied onto the wound, while a little imperfect wound closure was also noticed yet at day 15 post-treatment. Strikingly, sucrose laurate solution and its dual and triple mixtures displayed potentiated healing responses with almost the entire closure of wounds at the end of the experiment.

According to the onset of healing response results, solutions of single components (*i.e.*, sucrose laurate, lactose linoleate, and lactose linolenate) displayed a remarkable rapid onset of healing response at 3 days after wounding (Figure 4). Their healing abilities were found to be significantly faster than those that belonged to chitosan and the marketed product Healosol® as well as the positive control of untreated wounds ($p < 0.05$). However, compared to solutions of single components, dual and triple combinations showed a much more potent acceleration of wound healing.

Notably, the time for 50% reduction of wound area was between 3 and 5 days, and 5 and 7 days after wound induction for solutions of tested single forms and marketed product were observed respectively (Figure 4A). Comparatively, more than 50% reduction in the wound area was achieved with rats treated with all dual and triple combinations at 3 days post-injury except chitosan and lactose linolenate combination that showed 50% wound contraction between 3 and 5 days (Figure 4A).

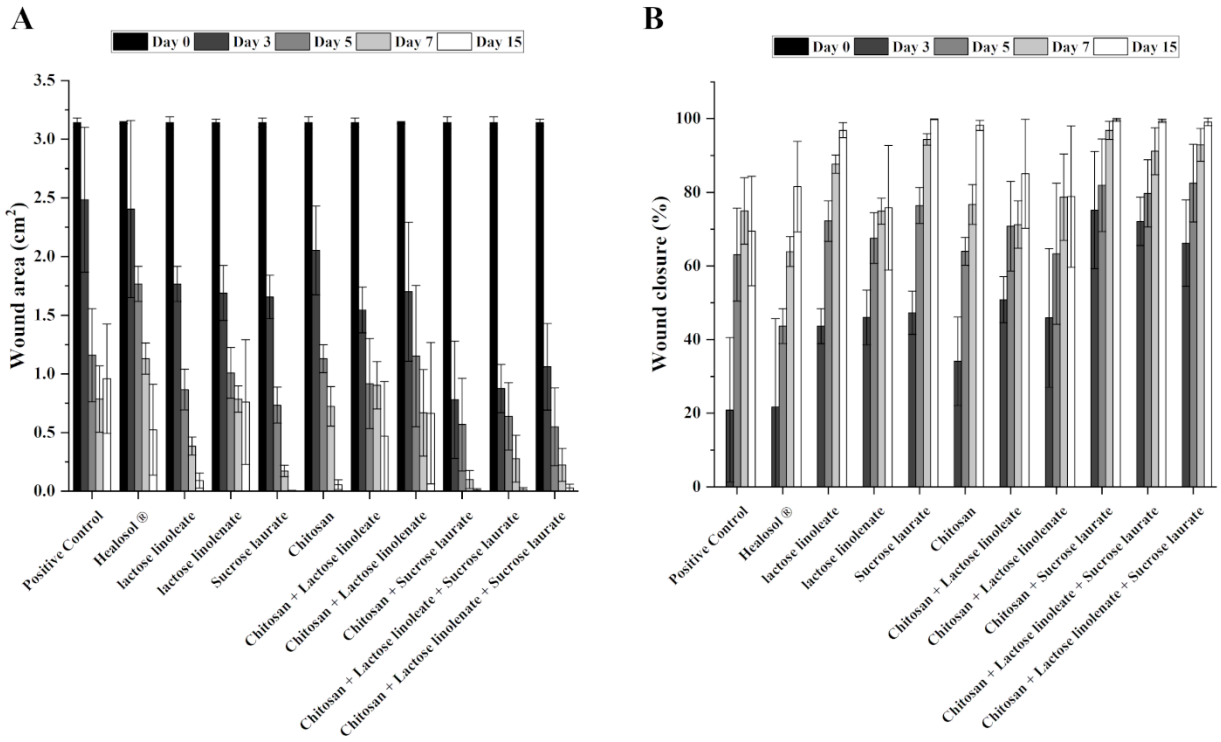

Figure 4. Effects of sugar derivatives and their combinations on wound area and on percent of wound closure as a function of time in different treatment groups. Data are presented as mean ± SEM (n = 6). (A) Wound area, (B) Wound closure.

It is worth mentioning that the wound closure in treated groups receiving chitosan, lactose linoleate, lactose linolenate solutions, and their combinations was lower than sucrose laurate treated groups. The lowest efficiency and incompletely healed tissue injuries were noticed with the rats treated with lactose linolenate, binary mixture of lactose linolenate and chitosan, and marketed product Healosol® showing only 78.84%, 84.79%, and 83.32% wound closure at the end of the treatment protocol (Figure 4B). On the other hand, the treated group receiving sucrose laurate solution and its mixed forms showed considerable restorative power of more than 90% wound closure in 7 days and wound recovery in 15 days post-injury.

To conclude, considering the comparison between the parallel treatments, sucrose laurate and its mixed forms were found to have the best efficiency in wound care among all the tested wound care forms in terms of acceleration of the cascade of wound healing adapt recovery of tissue injury.

3.7.2 Sugar-based esters and their combinations with chitosan resolved histopathological alterations induced by wound and increased collagen formation during wound healing

Histological examination of wound stained with H&E (Figure 5 and supplementary material Figure 4) showed normal histological structures of different skin layers in the control group with normal hair follicles and minimal inflammatory cells infiltrates and normal subcutaneous layer. On the other hand, persistent wide gab in the wound covered occasionally with scab from necrotic tissue depress with obvious loss and necrosis of underlying epidermal layer were recorded in the positive control (untreated) group, in marketed product Healosol® treated groups, chitosan treated group, in lactose linolenate treated groups and in the combination of chitosan with lactose linoleate treated group. These wounds were also filled with newly formed granulation tissue with abundant inflammatory cells infiltrates accompanied by fibroblastic proliferation, focal subepidermal hemorrhagic patches as well as newly formed blood vessels. However, positive control (untreated) group and marketed product Healosol® treated groups demonstrated minimal quantitative records of mature collagen fibers in dermal layer as shown in masson's trichrome stained tissue sections of all samples.

On the contrary, sucrose laurate or its combination with chitosan or the triple combination of chitosan/sucrose laurate/lactose linoleate treated groups showed more accelerated wound healing process with complete epidermal re-epithelialization and minimal persistence of subepidermal granulation tissue with few inflammatory cells infiltrates as well as higher records of mature dermal collagen fibers formation as shown in Masson's trichrome stained sections.

Similarly, lactose linoleate showed a more accelerated wound healing process with a wide wound gap filled with granulation tissue with abundant fibroblastic activity and few inflammatory cells infiltrates. Associated with complete epidermal re-epithelialization. However, lower records of mature dermal collagen fibers formation were shown in Masson's trichrome stained sections (Figure 6 and supplementary material Figure 5).

Interestingly, our results showed that the sucrose laurate treated group and its combination with chitosan treated groups showedmore accelerated new hair follicles formation.

Triple combination of chitosan/sucrose laurate/lactose linoleate showed complete epidermal re-epithelialization and minimal persistence of subepidermal granulation tissue with minimal inflammatory cells infiltrates. However, less accelerated records of mature dermal collagen fibers formation were shown in Masson's trichrome stained sections (Figure 7). Moreover, more abundant records of newly regenerated hair follicles were recorded (Supplementary material Table 9).

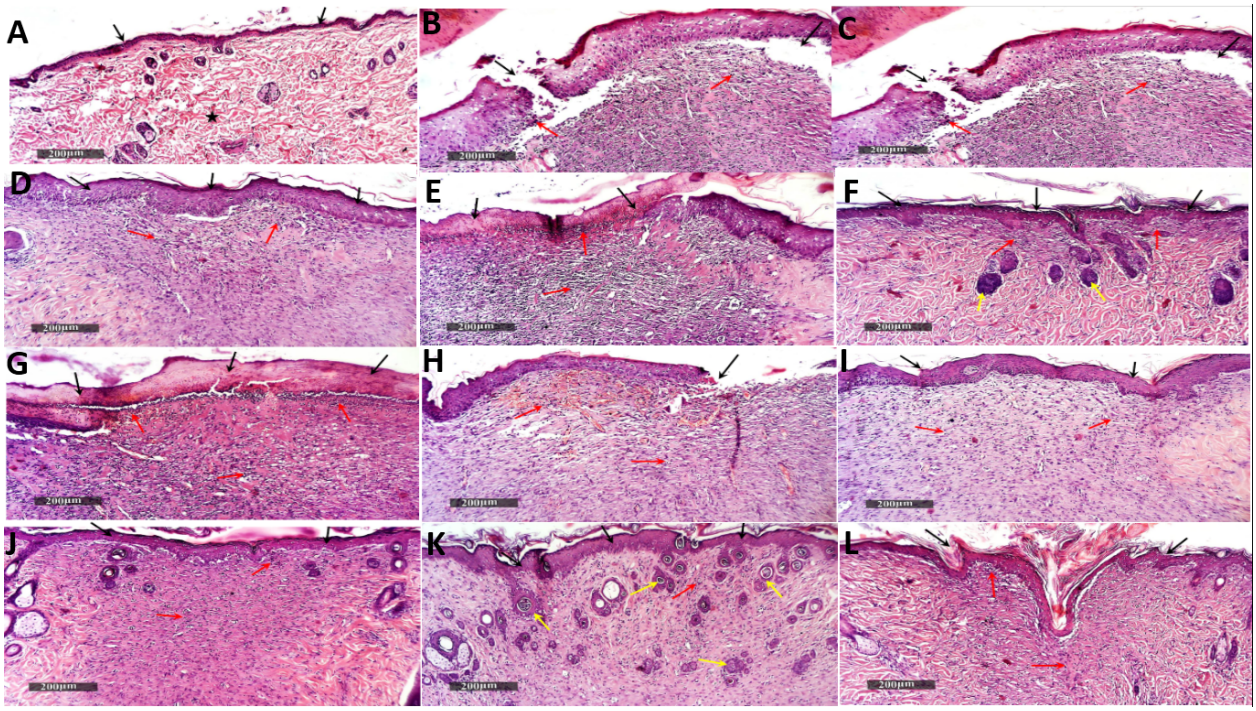

Figure 5. Effects of sugar derivatives and their combinations on histological alteration induced by wound: photomicrographs of H&E stained sections of wound (scale bars 200 µm) (n=6) depicting:

(A) Control group shows demonstrated normal histological structures of different skin layers including apparent intact epidermal layer with intact covering epithelium (arrow), intact dermal layer with normally distributed collagen fibers (star), hair follicles and minimal inflammatory cells infiltrates, and normal subcutaneous layer were recorded.

(B) Positive control (untreated wound) group shows the persistence of wide area of wound gab covered occasionally with scab from necrotic tissue depress with obvious loss and necrosis of underlying epidermal layer (arrow) and filled with newly formed granulation tissue with abundant inflammatory cells infiltrates (red arrow), fibroblastic proliferation, focal subepidermal hemorrhagic patches as well as newly formed blood vessels.

(C) Healosol® treated group shows the persistence of wide area of wound gab covered occasionally with scab from necrotic tissue depress with obvious loss, necrosis of underlying epidermal layer with focal separation (arrow) with abundant granulation tissue rich with inflammatory cells infiltrates (red arrow), fibroblastic proliferation, focal subepidermal hemorrhagic patches as well as newly formed blood vessels.

(D) Lactose linoleate treated group shows accelerated wound healing process with complete epidermal re-epithelialization (arrow) and minimal persistence of subepidermal granulation tissue with few inflammatory cells infiltrates (red arrow).

(E) Lactose linolenate treated group showspersistence of wide area of wound gab covered occasionally with scab from necrotic tissue depress with obvious loss and necrosis of underlying epidermal layer (arrow) and filled with newly formed granulation tissue with abundant inflammatory cells infiltrates (red arrow), fibroblastic proliferation, focal subepidermal hemorrhagic patches as well as newly formed blood vessels.

(F) Sucrose laurate treated group shows accelerated wound healing process were observed with complete epidermal re-epithelialization (arrow) and minimal persistence of subepidermal granulation tissue with few inflammatory cells infiltrates (red arrow). Moreover, newly regenerated hair follicles were shown (yellow arrow).

(G) Chitosan treated group showspersistence of a wide area of wound gab covered occasionally with scab from necrotic tissue depress with obvious loss and necrosis of underlying epidermal layer (arrow) and filled with newly formed

granulation tissue with abundant inflammatory cells infiltrates (red arrow), fibroblastic proliferation, focal subepidermal hemorrhagic patches as well as newly formed blood vessels.

(H) Chitosan/lactose linoleate treated group showspersistence of a wide area of wound gab covered occasionally with scab from necrotic tissue depress with obvious loss, necrosis of underlying epidermal layer with focal separation (arrow) with abundant granulation tissue rich with inflammatory cells infiltrates (red arrow), fibroblastic proliferation, focal subepidermal hemorrhagic patches as well as newly formed blood vessels.

(I) Chitosan/lactose linolenate treated group showsmore accelerated wound healing process with wide wound gap filled with granulation tissue with abundant fibroblastic activity and few inflammatory cells infiltrates (red arrow), complete epidermal re-epithelialization (arrow).

(J) Chitosan/sucrose laurate treated group showsaccelerated wound healing process was observed with complete epidermal re-epithelialization (arrow) and minimal persistence of subepidermal granulation tissue with few inflammatory cells infiltrates (red arrow). Moreover, a higher rate of mature collagen fibers formation was recorded with more accelerated new hair follicles formation (yellow arrow).

(K) Chitosan/lactose linoleate/sucrose laurate treated group shows complete epidermal re-epithelialization (arrow) and minimal persistence of subepidermal granulation tissue with minimal inflammatory cells infiltrates (red arrow). Moreover; more abundant records of newly regenerated hair follicles (yellow arrow) were shown.

(L) Chitosan/lactose linolenate/sucrose laurate treated group shows accelerated wound healing process was observed with complete epidermal re-epithelialization (arrow) and minimal persistence of subepidermal granulation tissue with few inflammatory cells infiltrates (red arrow).

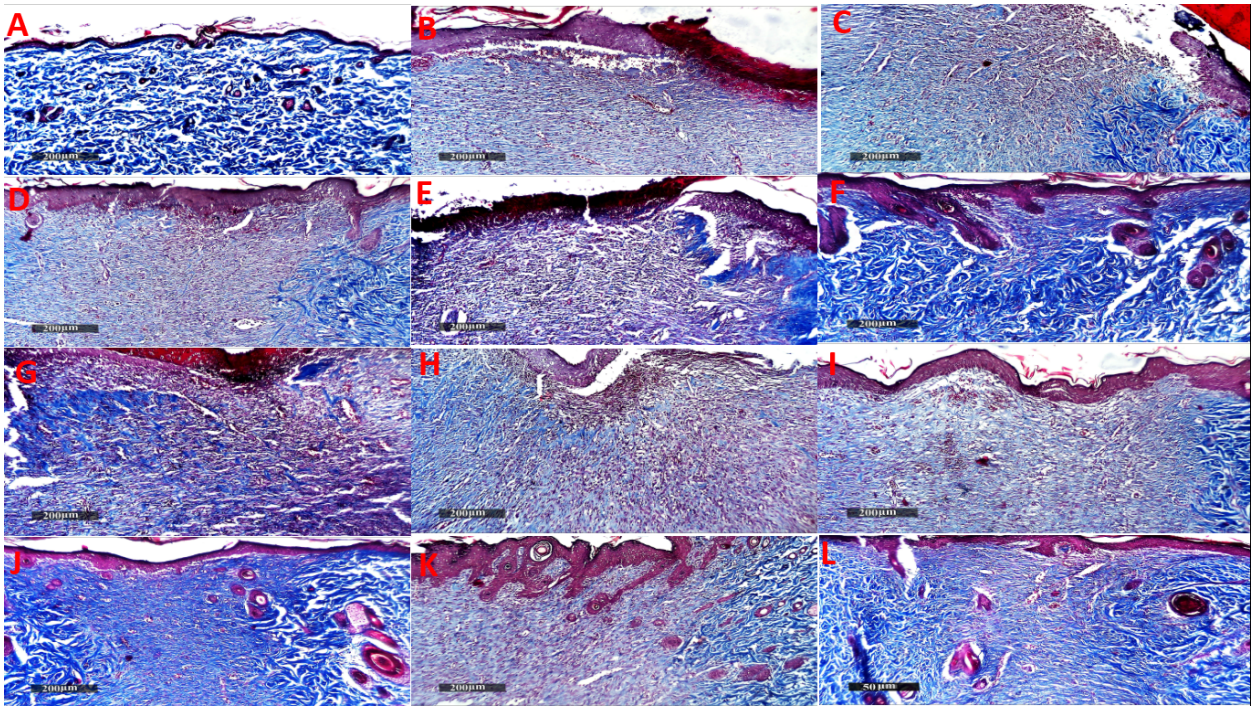

Figure 6. Effects of sugar derivatives and their combinations on collagen expression in different treatment groups: (A) Control group, (B) Positive control (untreated wound) group, (C) Healosol® treated group, (D) Lactose linoleate treated group, (E) Lactose linolenate treated group, (F) Sucrose laurate treated group, (G) Chitosan treated group, (H) Chitosan/lactose linoleate treated group, (I) Chitosan/lactose linolenate treated group, (J) Chitosan/sucrose

lauratetreated group, (K) Chitosan/lactose linoleate/sucrose laurate treated group, (L) Chitosan/lactose linolenate/sucrose laurate treated group. (Scale bars 200µm) (n=6).

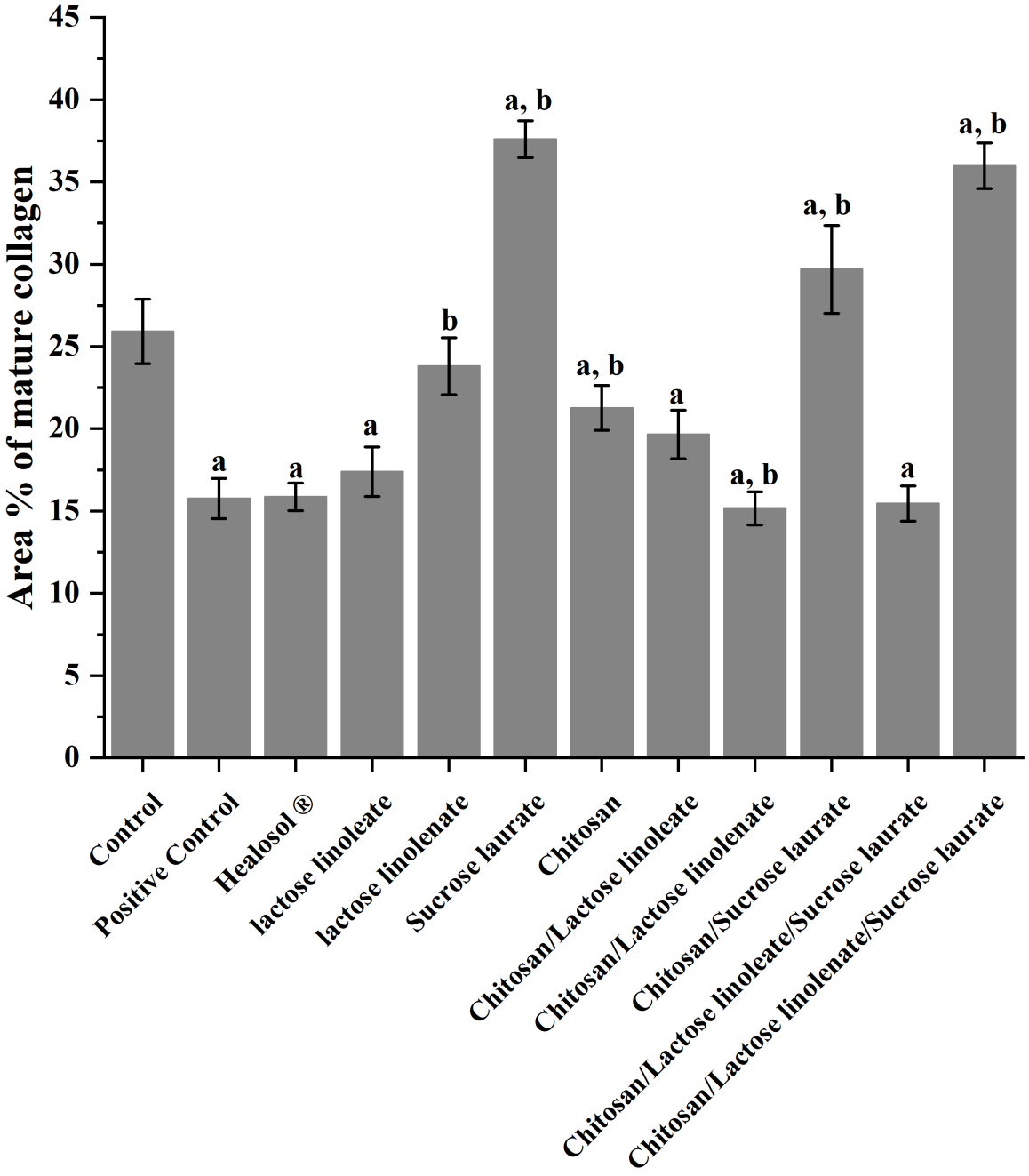

Figure 7. Determination of area percentage of reactive collagen fibers to Masson's trichrome stain. Data are presented as mean ± SEM (n = 6). Statistical Analysis was performed using one-way ANOVA followed by Tukey's test as post-hoc test. a) Significantly different from Control group at $p < 0.05$. b) Significantly different from Positive control group at $p < 0.05$

3.7.3 Sugar-based esters and their combinations with chitosan restored disrupted Wnt/β-catenin signaling pathwayduring wound healing

Knowing that the canonical Wnt/β-catenin pathway is intricately involved in wound, inflammation proliferation, remodeling regulation, and control of stem cells (Zhang et al., 2018), our study aimed to investigate the effect of our biomaterials on the expression of key factors in Wnt/β-catenin signaling pathway. In fact, Wnt signaling is initiated by binding of Wnt ligands (as Wnt-1) to their receptors, resulting in a cytoplasmic and nuclear increase of β-catenin which ultimately activates target genes (as c-Myc) that function in many cellular processes (Shi et al., 2015). Whereas, previous reports associated the important role played by c-myc in stimulating the epidermal stem cells to accelerate wound healing (Waikel et al., 2001), thus its downregulation can induce delayed wound healing (Frye et al., 2003). Furthermore, β-catenin was reported to be associated with epidermal cell proliferation, differentiation, and migration (Zhang et al., 2012), and thus its increase accelerates wound healing.Because Wnt-1 is a Wnt ligand, it was reported to activate the β-catenin-dependent Wnt pathway (Kiesslich et al., 2010) and its increase was found to regulate wound repair and regeneration of the skin (Lim and Nusse, 2013). On the other side, the Wnt-2 ligand was associated with skin fibrosis (Bayle et al., 2008). Whereas, its downregulation was reported to block fibrosis in human keloid fibroblast (Cai et al., 2017).

Our results showed increased gene expressions of Wnt-1, c-myc and β-catenin in treated groups receiving sucrose laurate and lactose linoleate both in single and combined formulations as compared to the untreated wound group (positive control). However, groups treated with single lactose linolenate showed a significant increase in c-myc gene expression with no significant increase in Wnt-1 and β-catenin genes expression as compared to untreated wound group (positive control). Alongside, no significant increase was detected in Wnt-1, c-myc and β-catenin genes expression in chitosan or in marketed product Healosol® as compared to untreated wound group (positive control). Meanwhile, chitosan showed significant decrease in Wnt-1 gene expression as compared to unwounded group (negative control). Similarly, marketed product Healosol® showed significant decrease in β-catenin gene expression as compared to unwounded group (negative control), which highlights the superior beneficial effects of our biomaterials in either single or combined formulations especially for sucrose laurate and lactose linoleate. Noteworthy, sucrose laurate in single and combined formulations showed the highest increase in Wnt-1, c-myc, and β-catenin genes expression. On the other side, a significant decrease in Wnt-2 gene expression was reported in sucrose laurate single or combined formulations as compared to the untreated wound group (positive control). Meanwhile, the marketed product Healosol® showed a significant increase in Wnt-2 gene expression as compared to the unwounded group (negative control) (Figure 8).

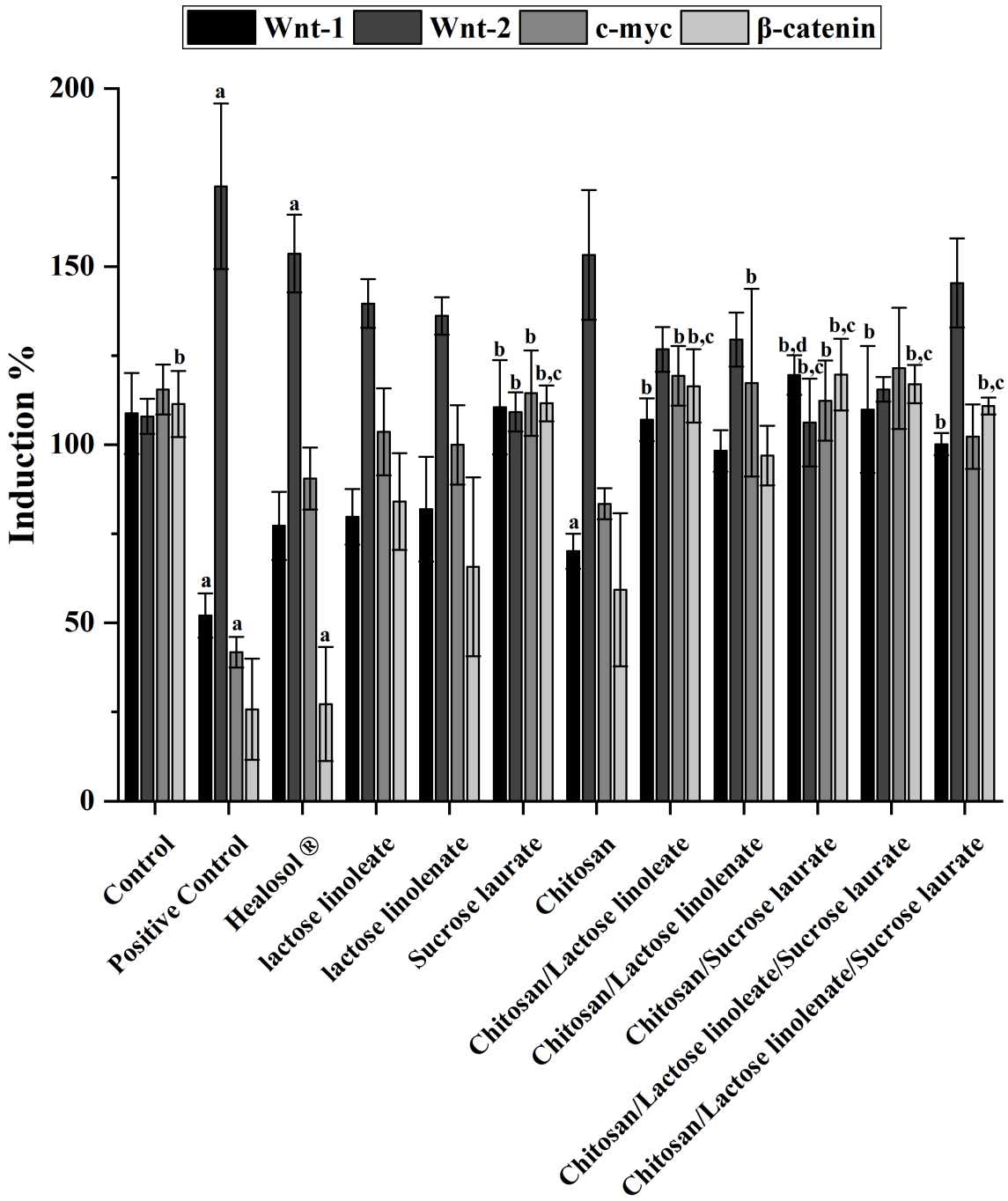

Figure 8. Effects of sugar derivatives and their combinations on Wnt/β-catenin signaling genes expression genes. Data are presented as mean ± SEM (n = 6).tatistical Analysis was performed using one-way ANOVA followed by Tukey's test as post-hoc test. a) Significantly different from Control group at $p < 0.05$; b) Significantly different from Positive control group at $p < 0.05$; c) Significantly different from Halosol® group at $p < 0.05$; d) Significant different from Chitosan group at $p < 0.05$.

4. CONCLUSIONS

The development and application of new biocompatible materials is a main challenge for formulation scientists. Ideal wound dressing formulas must possess antioxidant, anti-inflammatory, and antimicrobial properties and must induce skin regenerative activities. Here, we have been able to synthesize and characterize new lactose-based sugar esters via a mild Steglich esterification. Sucrose laurate, chitosan and the synthesized lactose linoleate and lactose linolenate were tested *in vitro* and *in vivo* to evaluate their properties alone or as mixtures. They showed high biocompatibility both *in vitro* and *in vivo,* coupled with antioxidant and anti-inflammatory effects, accompanied by antimicrobial and antifungal activities. More specifically, the sugar esters (*i.e.*, sucrose laurate and sucrose linoleate) and chitosan combinations showed a wound closure above 90% in male Wistar albino rats linked with the restoration of the Wnt/β-catenin signaling. This signaling modulates the inflammatory, and the oxidative stress states, and it controls stem cells to induce epidermal cell proliferation which accelerates both wound healing and skin regeneration. This innovative combination of biomaterials applied in wound dressing could effectively break new ground in skin wound care.

CRediT Authorship

MT and EE: Investigation, data curation, formal analysis, methodology, visualization, and writing - original draft;

MOE, SB, RC, MV, LP, FP, BC, MS, AD, SL: Formal analysis, investigation, methodology, writing - review & editing;

MES, LC: Conceptualization, experimental design, supervision, data curation, writing - review & editing and funding acquisition.

Conflicts of interest

The authors declare that they have no known competing financial interests or personal relationships that could have appeared to influence the work reported in this paper.

Funding

This work was supported by Università di Urbino Carlo Bo, Urbino (PU), Italy (grant DISB_CASETTARI_ATENEO_SALUTE2018)

5. REFERENCES

Abd El-Hack, M.E., El-Saadony, M.T., Shafi, M.E., Zabermawi, N.M., Arif, M., Batiha, G.E., Khafaga, A.F., Abd El-Hakim, Y.M., Al-Sagheer, A.A., 2020. Antimicrobial and antioxidant properties of chitosan and its derivatives and their applications: A review. Int. J. Biol. Macromol. 164, 2726–2744. https://doi.org/10.1016/J.IJBIOMAC.2020.08.153

Al-Sayed, E., Michel, H.E., Khattab, M.A., El-Shazly, M., Singab, A.N., 2020. Protective role of casuarinin from melaleuca leucadendra against ethanol-induced gastric ulcer in rats. Planta Med. 86, 32–44. https://doi.org/10.1055/a-1031-7328

Aldalaen, S., Nasr, M., El-Gogary, R.I., 2020. Angiogenesis and collagen promoting nutraceutical-loaded nanovesicles for wound healing. J. Drug Deliv. Sci. Technol. 56, 101548. https://doi.org/10.1016/j.jddst.2020.101548

Amini-Nik, S., Cambridge, E., Yu, W., Guo, A., Whetstone, H., Nadesan, P., Poon, R., Hinz, B., Alman, B.A., 2014. β-Catenin-regulated myeloid cell adhesion and migration determine wound healing. J. Clin. Invest. 124, 2599–2610. https://doi.org/10.1172/JCI62059

Anstead, G.M., Hart, L.M., Sunahara, J.F., Liter, M.E., 1996. Phenytoin in wound healing. Ann. Pharmacother. 30, 768–775. https://doi.org/10.1177/106002809603000712

Bayle, J., Fitch, J., Jacobsen, K., Kumar, R., Lafyatis, R., Lemaire, R., 2008. Increased expression of Wnt2 and SFRP4 in Tsk mouse skin: Role of Wnt signaling in altered dermal fibrillin deposition and systemic sclerosis. J. Invest. Dermatol. 128, 871–881. https://doi.org/10.1038/sj.jid.5701101

Bryan, N.S., Grisham, M.B., 2007. Methods to detect nitric oxide and its metabolites in biological samples. Free Radic. Biol. Med. 43, 645–647. https://doi.org/10.1016/j.freeradbiomed.2007.04.026

Cai, Y., Zhu, S., Yang, W., Pan, M., Wang, C., Wu, W., 2017. Downregulation of β-catenin blocks fibrosis via Wnt2 signaling in human keloid fibroblasts. Tumor Biol. 39, 1010428317707423. https://doi.org/10.1177/1010428317707423

Campana, R., Merli, A., Verboni, M., Biondo, F., Favi, G., Duranti, A., Lucarini, S., 2019. Synthesis and evaluation of saccharide-based aliphatic and aromatic esters as antimicrobial and antibiofilm agents. Pharmaceuticals 12, 186. https://doi.org/10.3390/ph12040186

Catalani, S., Palma, F., Battistelli, S., Benedetti, S., 2017a. Oxidative stress and apoptosis induction in human thyroid carcinoma cells exposed to the essential oil from Pistacia lentiscus aerial parts. PLoS One 12, e0172138. https://doi.org/10.1371/journal.pone.0172138

Catalani, S., Palma, F., Battistelli, S., Nuvoli, B., Galati, R., Benedetti, S., 2017b. Reduced cell viability and apoptosis induction in human thyroid carcinoma and mesothelioma cells exposed

765 to cidofovir. Toxicol. Vitr. 41, 49–55. https://doi.org/10.1016/j.tiv.2017.02.008
766 Chang, S.H., Lin, Y.Y., Wu, G.J., Huang, C.H., Tsai, G.J., 2019. Effect of chitosan molecular
767 weight on anti-inflammatory activity in the RAW 264.7 macrophage model. Int. J. Biol.
768 Macromol. 131, 167–175. https://doi.org/10.1016/J.IJBIOMAC.2019.02.066
769 Chongsiriwatana, N.P., Patch, J.A., Czyzewski, A.M., Dohm, M.T., Ivankin, A., Gidalevitz, D.,
770 Zuckermann, R.N., Barron, A.E., 2008. Peptoids that mimic the structure, function, and
771 mechanism of helical antimicrobial peptides. Proc. Natl. Acad. Sci. U. S. A. 105, 2794–2799.
772 https://doi.org/10.1073/pnas.0708254105
773 Elmowafy, E., El-derany, M.O., Biondo, F., Tiboni, M., Casettari, L., 2020. Quercetin Loaded
774 Monolaurate Sugar Esters-Based Niosomes: Sustained Release and Mutual Antioxidant –
775 Hepatoprotective Interplay, Pharmaceutics 12, 143.
776 https://doi.org/10.3390/pharmaceutics12020143
777 Farabegoli, F., Scarpa, E.S., Frati, A., Serafini, G., Papi, A., Spisni, E., Antonini, E., Benedetti, S.,
778 Ninfali, P., 2017. Betalains increase vitexin-2-O-xyloside cytotoxicity in CaCo-2 cancer cells.
779 Food Chem. 218, 356–364. https://doi.org/10.1016/j.foodchem.2016.09.112
780 Feng, P., Luo, Y., Ke, C., Qiu, H., Wang, W., Zhu, Y., Hou, R., Xu, L., Wu, S., 2021. Chitosan-
781 Based Functional Materials for Skin Wound Repair: Mechanisms and Applications. Front.
782 Bioeng. Biotechnol. 9, 650598. https://doi.org/10.3389/fbioe.2021.650598
783 Ferrer, M., Perez, G., Plou, F.J., Castell, J.V., Ballesteros, A., 2005. Antitumour activity of fatty
784 acid maltotriose esters obtained by enzymatic synthesis. Biotechnol. Appl. Biochem. 42, 35.
785 https://doi.org/10.1042/ba20040122
786 Frye, M., Gardner, C., Li, E.R., Arnold, I., Watt, F.M., 2003. Evidence that Myc activation depletes
787 the epidermal stem cell compartment by modulating adhesive interactions with the local
788 microenvironment. Development. https://doi.org/10.1242/dev.00462
789 Guan, Y., Chen, H., Zhong, Q., 2019. Nanoencapsulation of caffeic acid phenethyl ester in sucrose
790 fatty acid esters to improve activities against cancer cells. J. Food Eng. 246, 125–133.
791 https://doi.org/10.1016/j.jfoodeng.2018.11.008
792 Gumel, A.M., Annuar, M.S.M., Heidelberg, T., Chisti, Y., 2011. Lipase mediated synthesis of sugar
793 fatty acid esters. Process Biochem. 46, 2079–2090.
794 https://doi.org/10.1016/j.procbio.2011.07.021
795 Guth, F., Schiffter, H.A., Kolter, K., 2013. Novel excipients-from concept to launch. Chim. Oggi-
796 Chem. Today 31, 78–81.
797 Hough, L., Richardson, A.C., Thelwall, L.A.W., 1979. Reaction of lactose with 2,2-
798 dimethoxypropane: a tetraacetal of novel structure. Carbohydrate Res. 75, C11–C12.

https://doi.org/10.1016/S0008-6215(00)84663-7
Hu, H., Zhao, P., Liu, J., Ke, Q., Zhang, C., Guo, Y., Ding, H., 2018. Lanthanum phosphate/chitosan scaffolds enhance cytocompatibility and osteogenic efficiency via the Wnt/β-catenin pathway. J. Nanobiotechnol. 16, 98. https://doi.org/10.1186/s12951-018-0411-9
Kale, S.S., Akamanchi, K.G., 2016. Trehalose Monooleate: A Potential Antiaggregation Agent for Stabilization of Proteins. Mol. Pharm. 13, 4082–4093. https://doi.org/10.1021/acs.molpharmaceut.6b00686
Khan, M.A., Mujahid, M., 2019. A review on recent advances in chitosan based composite for hemostatic dressings. Int. J. Biol. Macromol. 124,138–147. https://doi.org/10.1016/j.ijbiomac.2018.11.045
Kiesslich, T., Alinger, B., Wolkersdörfer, G.W., Ocker, M., Neureiter, D., Berr, F., 2010. Active Wnt signalling is associated with low differentiation and high proliferation in human biliary tract cancer in vitro and in vivo and is sensitive to pharmacological inhibition. Int. J. Oncol. 36, 49–58. https://doi.org/10.3892/ijo_00000474
Kim, S., Ng, W.K., Shen, S., Dong, Y., Tan, R.B.H., 2009. Phase behavior, microstructure transition, and antiradical activity of sucrose laurate/propylene glycol/the essential oil of Melaleuca alternifolia/water microemulsions. Colloids Surfaces A Physicochem. Eng. Asp. 348, 289–297. https://doi.org/10.1016/J.COLSURFA.2009.07.043
Klang, V., Novak, A., Wirth, M., Valenta, C., 2013. Semi-Solid o/w Emulsions Based on Sucrose Stearates: Influence of Oil and Surfactant Type on Morphology and Rheological Properties. J. Dispers. Sci. Technol. 34, 322–333. https://doi.org/10.1080/01932691.2012.666187
Krawczyk, J., 2018. Solid Wettability Modification via Adsorption of Antimicrobial Sucrose Fatty Acid Esters and Some Other Sugar-Based Surfactants. Mol. 2018, 23, 1597. https://doi.org/10.3390/MOLECULES23071597
Lamouille, S., Xu, J., Derynck, R., 2014. Molecular mechanisms of epithelial-mesenchymal transition. Nat. Rev. Mol. Cell Biol. 15, 178–196. https://doi.org/10.1038/nrm3758
Lim, X., Nusse, R., 2013. Wnt signaling in skin development, homeostasis, and disease. Cold Spring Harb. Perspect. Biol. 5, a008029. https://doi.org/10.1101/cshperspect.a008029
Lucarini, S., Fagioli, L., Campana, R., Cole, H., Duranti, A., Baffone, W., Vllasaliu, D., Casettari, L., 2016. Unsaturated fatty acids lactose esters: cytotoxicity, permeability enhancement and antimicrobial activity. Eur. J. Pharm. Biopharm. 107, 88–96. https://doi.org/10.1016/j.ejpb.2016.06.022
Lucarini, S., Fagioli, L., Cavanagh, R., Liang, W., Perinelli, D.R., Campana, M., Stolnik, S., Lam, J.K.W., Casettari, L., Duranti, A., 2018. Synthesis, structure–activity relationships and in vitro

toxicity profile of lactose-based fatty acid monoesters as possible drug permeability enhancers. Pharmaceutics 10, 81. https://doi.org/10.3390/pharmaceutics10030081

Lukic, M., Pantelic, I., Savic, S., 2016. An overview of novel surfactants for formulation of cosmetics with certain emphasis on acidic active substances. Tenside, Surfactants, Deterg. 53, 7–19. https://doi.org/10.3139/113.110405

Manzoor, M., Singh, J., Bandral, J.D., Gani, A., Shams, R., 2020. Food hydrocolloids: Functional, nutraceutical and novel applications for delivery of bioactive compounds. Int. J. Biol. Macromol. 165, 554–567. https://doi.org/10.1016/j.ijbiomac.2020.09.182

Marathe, S.J., Shah, N.N., Singhal, R.S., 2020. Enzymatic synthesis of fatty acid esters of trehalose: Process optimization, characterization of the esters and evaluation of their bioactivities. Bioorg. Chem. 94, 103460. https://doi.org/10.1016/j.bioorg.2019.103460

Mari, G., Catalani, S., Antonini, E., De Crescentini, L., Mantellini, F., Santeusanio, S., Lombardi, P., Amicucci, A., Battistelli, S., Benedetti, S., Palma, F., 2018. Synthesis and biological evaluation of novel heteroring-annulated pyrrolino-tetrahydroberberine analogues as antioxidant agents. Bioorg. Med. Chem. 26, 5037–5044. https://doi.org/10.1016/j.bmc.2018.08.038

Matica, M.A., Aachmann, F.L., Tøndervik, A., Sletta, H., Ostafe, V., 2019. Chitosan as a wound dressing starting material: Antimicrobial properties and mode of action. Int. J. Mol. Sci. https://doi.org/10.3390/ijms20235889

Matin, M., Roshid, M.H., Bhattacharjee, S., Azad, A., 2020. PASS Predication, Antiviral, in vitro Antimicrobial, and ADMET Studies of Rhamnopyranoside Esters. Med. Res. Arch. 8. https://doi.org/10.18103/mra.v8i7.2165

McCartney, F., Perinelli, D.R., Tiboni, M., Cavanagh, R., Lucarini, S., Filippo Palmieri, G., Casettari, L., Brayden, D.J., 2021. Permeability-enhancing effects of three laurate-disaccharide monoesters across isolated rat intestinal mucosae. Int. J. Pharm. 601, 120593. https://doi.org/10.1016/j.ijpharm.2021.120593

Mohan, K., Ganesan, A.R., Muralisankar, T., Jayakumar, R., Sathishkumar, P., Uthayakumar, V., Chandirasekar, R., Revathi, N., 2020. Recent insights into the extraction, characterization, and bioactivities of chitin and chitosan from insects. Trends Food Sci. Technol. 105, 17–42. https://doi.org/10.1016/j.tifs.2020.08.016

Neises, B., Steglich, W., 1978. Simple Method for the Esterification of Carboxylic Acids. Angew. Chemie Int. Ed. English 17, 522–524. https://doi.org/10.1002/anie.197805221

Neta, N. do A.S., Santos, J.C.S. dos, Sancho, S. de O., Rodrigues, S., Gonçalves, L.R.B., Rodrigues, L.R., Teixeira, J.A., 2012. Enzymatic synthesis of sugar esters and their potential

867 as surface-active stabilizers of coconut milk emulsions. Food Hydrocoll. 27, 324–331.
868 https://doi.org/10.1016/j.foodhyd.2011.10.009
869 Neta, N.S., Teixeira, J.A., Rodrigues, L.R., 2015. Sugar Ester Surfactants: Enzymatic Synthesis and
870 Applications in Food Industry. Crit. Rev. Food Sci. Nutr. 55, 595–610.
871 https://doi.org/10.1080/10408398.2012.667461
872 Pérez, B., Anankanbil, S., Guo, Z., 2017. Synthesis of Sugar Fatty Acid Esters and Their Industrial
873 Utilizations, in: Fatty Acids. Elsevier, pp. 329–354. https://doi.org/10.1016/b978-0-12-
874 809521-8.00010-6
875 Perinelli, D.R., Lucarini, S., Fagioli, L., Campana, R., Vllasaliu, D., Duranti, A., Casettari, L., 2018.
876 Lactose oleate as new biocompatible surfactant for pharmaceutical applications. Eur. J. Pharm.
877 Biopharm. 124, 55–62. https://doi.org/10.1016/j.ejpb.2017.12.008
878 Saberian, M., Seyedjafari, E., Zargar, S.J., Mahdavi, F.S., Sanaei-rad, P., 2021. Fabrication and
879 characterization of alginate/chitosan hydrogel combined with honey and aloe vera for wound
880 dressing applications. J. Appl. Polym. Sci. 138, 1–15. https://doi.org/10.1002/app.51398
881 Saltarelli, R., Palma, F., Gioacchini, A.M., Calcabrini, C., Mancini, U., De Bellis, R., Stocchi, V.,
882 Potenza, L., 2019. Phytochemical composition, antioxidant and antiproliferative activities and
883 effects on nuclear DNA of ethanolic extract from an Italian mycelial isolate of Ganoderma
884 lucidum. J. Ethnopharmacol. 231, 464–473. https://doi.org/10.1016/j.jep.2018.11.041
885 Sanchez, M.C., Lancel, S., Boulanger, E., Neviere, R., 2018. Targeting oxidative stress and
886 mitochondrial dysfunction in the treatment of impaired wound healing: A systematic review.
887 Antioxidants. 7, 98. https://doi.org/10.3390/antiox7080098
888 Schiefelbein, L., Keller, M., Weissmann, F., Luber, M., Bracher, F., Frieß, W., 2010. Synthesis ,
889 characterization and assessment of suitability of trehalose fatty acid esters as alternatives for
890 polysorbates in protein formulation. Eur. J. Pharm. Biopharm. 76, 342–350.
891 https://doi.org/10.1016/j.ejpb.2010.08.012
892 Sferrazza, G., Corti, M., Brusotti, G., Pierimarchi, P., Temporini, C., Serafino, A., Calleri, E., 2020.
893 Nature-derived compounds modulating Wnt/β-catenin pathway: a preventive and therapeutic
894 opportunity in neoplastic diseases. Acta Pharm. Sin. B. 10, 1814–1834.
895 https://doi.org/10.1016/j.apsb.2019.12.019
896 Shaw, J., Hughes, C.M., Lagan, K.M., Bell, P.M., 2007. The clinical effect of topical phenytoin on
897 wound healing: A systematic review. Br. J. Dermatol. 157, 997–1004.
898 https://doi.org/10.1111/j.1365-2133.2007.08160.x
899 Shi, Y., Shu, B., Yang, R., Xu, Y., Xing, B., Liu, J., Chen, L., Qi, S., Liu, X., Wang, P., Tang, J.,
900 Xie, J., 2015. Wnt and Notch signaling pathway involved in wound healing by targeting c-Myc

and Hes1 separately. Stem Cell Res. Ther. 6, 1–13. https://doi.org/10.1186/s13287-015-0103-4
Szuts, A., Láng, P., Ambrus, R., Kiss, L., Deli, M.A., Szabó-Révész, P., 2011. Applicability of sucrose laurate as surfactant in solid dispersions prepared by melt technology. Int. J. Pharm. 410, 107–110. https://doi.org/10.1016/j.ijpharm.2011.03.033
Teng, Y., Stewart, S.G., Hai, Y.W., Li, X., Banwell, M.G., Lan, P., 2021. Sucrose fatty acid esters: synthesis, emulsifying capacities, biological activities and structure-property profiles. Crit. Rev. Food Sci. Nutr. 61, 3297–3317. https://doi.org/10.1080/10408398.2020.1798346
Tiboni, M., Coppari, S., Casettari, L., Guescini, M., Colomba, M., Fraternale, D., Gorassini, A., Verardo, G., Ramakrishna, S., Guidi, L., Di Giacomo, B., Mari, M., Molinaro, R., Albertini, M.C., 2021. Prunus spinosa extract loaded in biomimetic nanoparticles evokes in vitro anti-inflammatory and wound healing activities. Nanomaterials 11, 1–14. https://doi.org/10.3390/nano11010036
Wagh, A., Shen, S., Shen, F.A., Miller, C.D., Walsha, M.K., 2012. Effect of lactose monolaurate on pathogenic and nonpathogenic bacteria. Appl. Environ. Microbiol. 78, 3465–3468. https://doi.org/10.1128/AEM.07701-11
Waikel, R.L., Kawachi, Y., Waikel, P.A., Wang, X.J., Roop, D.R., 2001. Deregulated expression of c-Myc depletes epidermal stem cells. Nat. Genet. 28, 165–168. https://doi.org/10.1038/88889
Yang, H.L., Tsai, Y.C., Korivi, M., Chang, C.T., Hseu, Y.C., 2017. Lucidone Promotes the Cutaneous Wound Healing Process via Activation of the PI3K/AKT, Wnt/β-catenin and NF-κB Signaling Pathways. Biochim. Biophys. Acta - Mol. Cell Res. 1864, 151–168. https://doi.org/10.1016/j.bbamcr.2016.10.021
Zhang, C., Chen, P., Fei, Y., Liu, B., Ma, K., Fu, X., Zhao, Z., Sun, T., Sheng, Z., 2012. Wnt/β-catenin signaling is critical for dedifferentiation of aged epidermal cells in vivo and in vitro. Aging Cell 11, 14–23. https://doi.org/10.1111/j.1474-9726.2011.00753.x
Zhang, H., Nie, X., Shi, X., Zhao, J., Chen, Y., Yao, Q., Sun, C., Yang, J., 2018. Regulatory mechanisms of the Wnt/β-catenin pathway in diabetic cutaneous ulcers. Front. Pharmacol. https://doi.org/10.3389/fphar.2018.01114
Zhang, X., Wei, W., Cao, X., Feng, F., 2015. Characterization of enzymatically prepared sugar medium-chain fatty acid monoesters. J. Sci. Food Agric. 95, 1631–1637. https://doi.org/10.1002/jsfa.6863
Zhao, L., Zhang, H., Hao, T., Li, S., 2015. In vitro antibacterial activities and mechanism of sugar fatty acid esters against five food-related bacteria. Food Chem. 187, 370–377. https://doi.org/10.1016/j.foodchem.2015.04.108
Zheng, Y., Zheng, M., Ma, Z., Xin, B., Guo, R., Xu, X., 2015. Sugar Fatty Acid Esters, in: Polar

935 Lipids: Biology, Chemistry, and Technology. Elsevier Inc., pp. 215–243.
936 https://doi.org/10.1016/B978-1-63067-044-3.50012-1
937